The Canadian Mineralogist
Vol. 40, pp. 47-65 (2002)

FLUID INCLUSIONS IN LATE-STAGE Pb–Mn–As–Sb MINERAL ASSEMBLAGES IN THE LÅNGBAN DEPOSIT, BERGSLAGEN, SWEDEN

ERIK JONSSON[§]

Department of Mineralogy, Swedish Museum of Natural History, Box 50007, SE-104 05 Stockholm, and Department of Geology and Geochemistry, Stockholm University, SE-106 91 Stockholm, Sweden

CURT BROMAN

Department of Geology and Geochemistry, Stockholm University, SE-106 91 Stockholm, Sweden

Abstract

The Långban deposit in the Paleoproterozoic Bergslagen ore province in southwestern central Sweden is well known for its complex and unique mineralogy. The largest number of exotic species occur in late-stage Pb–Mn–As–Sb-bearing fissures of disputed origin. Fluid inclusions in fissure-hosted allactite, barite, blixite, calcite, sarkinite, tilasite and finnemanite suggest a low-temperature near-surface formation at, or close to, atmospheric pressure, from aqueous $NaCl–CaCl_2–MgCl_2$ solutions of initially moderate salinity. Mineral formation started at temperatures of *ca.* 180°C, with the fluid evolving through reactions with Mn-oxide-bearing dolomites and a sequence of boiling events, initiated by repeated fracturing, at temperatures fluctuating between *ca.* 80 and 130°C. This main stage is characterized by precipitation of alternating species (*e.g.*, barite, calcite, allactite, native lead, pyrochroite), with solutions evolving further to heterogeneous high-salinity compositions at temperatures less than *ca.* 70°C. Late low-salinity inclusions formed through partial condensation of the expelled vapor phase. Continued formation of minerals (*e.g.*, arsenites, H_2O-rich arsenates) after the major boiling events is characterized by temperatures decreasing well below 70°C. The solutions responsible for the specific fissure-mineralization at Långban were introduced in a very shallow post-Svecokarelian brittle tectonic environment, in conjunction with a *ca.* 1 Ga tectonothermal episode, or possibly coupled to post-1.8-Ga granitic magmatism. The absence of similar mineralized systems of brittle fissures on a regional scale suggests that the metals in the Långban fissures were derived very locally from the pre-existing volcanic-exhalative mineralization and not introduced from an external source.

Keywords: Långban, ore deposit, fluid inclusions, allactite, barite, blixite, calcite, finnemanite, sarkinite, tilasite, Bergslagen, Sweden.

Sommaire

Le gisement de Långban, dans la province métallogénique paléoprotérozoïque de Bergslagen, dans le secteur sud-ouest central de la Suède, est reconnu pour ses assemblages complexes et uniques de minéraux. La majorité des espèces exotiques se trouvent dans les fissures tardives à Pb–Mn–As–Sb, d'origine controversée. Les inclusions fluides des minéraux déposés dans ces fissures, par exemple allactite, barite, blixite, calcite, sarkinite, tilasite et finnemanite, indiquent une faible température et une déposition à pression atmosphérique, ou presque, à partir de solutions contenant $NaCl–CaCl_2–MgCl_2$, de salinité intermédiaire, au moins au début. La formation de ces assemblages à débuté à environ 180°C, et les fluides ont évolué par réaction avec une séquence de dolomies manganifères et une série d'événements d'ébullition initiés par ouverture répétée de fractures à une température fluctuant entre 80 et 130°C. L'étape principale est marquée par la précipitation d'une alternance d'espèces (*e.g.*, barite, calcite, allactite, plomb natif, pyrochroïte), et par l'évolution progressive des solutions, devenues hétérogènes, vers une salinité plus élevée à une température inférieure à environ 70°C. Les inclusions tardives à faible salinité se sont formées par condensation partielle de la phase vapeur libérée. La formation continue de minéraux (*e.g.*, arsenites, arsenates riches en H_2O) après les événements d'ébullition a atteint des températures bien inférieures à 70°C. Les solutions responsables de cet épisode de minéralisation fissurale à Långban ont été introduites suite à un événement post-Svécokarélien impliquant une tectonique cassante liée à un épisode tectonothermique à environ 1 Ga, ou bien possiblement à un épisode de magmatisme granitique de moins de 1.8 Ga. A notre avis, l'absence de systèmes minéralisés semblables le long de fissures développées sur une échelle régionale montre

§ *E-mail address*: erik.jonsson@geo.su.se, curt.broman@geo.su.se

que les métaux des fissures à Långban ont une dérivation strictement locale à partir des minerais d'origine volcanique exhalative, et ne seraient donc pas introduits d'une source externe.

(Traduit par la Rédaction)

Most-clés: Långban, gîte minéral, inclusions fluides, allactite, barite, blixite, calcite, finnemanite, sarkinite, tilasite, Bergslagen, Suède.

Introduction

The Långban deposit, in Bergslagen, Sweden, is famous for its wealth of rare minerals (*e.g.*, Flink 1923, Magnusson 1930, Moore 1970, Nysten *et al.* 1999). In particular, late-stage fissures contain a mineralogically highly diversified and "exotic" set of species. Typical minerals in the fissures comprise oxychlorides, arsenates, arsenites and native metals. Of the approximately 270 known species from Långban, more than 50% are hosted by systems of late-stage fissures.

In spite of the great interest in Långban minerals, little has been published about the low-temperature genesis of Pb–Mn–As–Sb-bearing fissure mineralization in the Långban deposit, or other related occurrences in the Bergslagen ore province (the Långban-type deposits of Moore 1970). Fluid-inclusion studies have not been employed in any of these deposits, but could yield important clues to conditions of formation and processes. The objective of the present study is twofold. Firstly, we aim to provide new data to constrain the conditions of deposition for these unique assemblages, and secondly, we report for the first time microthermometric results from fluid inclusions hosted by some rare arsenate minerals. The results presented in this study also have important implications for a number of similar deposits in the Bergslagen ore province (*e.g.*, Harstigen, Jakobsberg, Nordmark; Moore 1970).

Background Information

The issue of the Långban fissure mineralization has been subject of debate for a long time, with varying theories about timing, P–T conditions and paragenetic evolution. Sjögren (1910) clearly noted "the secondary nature" of these assemblages. Aminoff (1918a, b) concluded that there was no distinct *hiatus* between the primary ore formation, metamorphism, and the later formation of fissure-type mineralization. He thus implied that the fissure minerals formed at relatively high pressure and temperature. The overall mineralogy, petrology and paragenesis of the Långban mines were further studied by Magnusson (1924, 1930). Magnusson (1930) considered the formation of "secondary" minerals, ranging from peak metamorphic assemblages to fissure-type mineralization, to be a sequence of events during a relatively short time-interval. Genetically relevant physicochemical and thermodynamic implications of specific mineral associations, in particular the important assemblage of native lead and pyrochroite, were presented by Boström (1965, 1967, 1981). Boström (1996) presented sulfur isotopic data, with resulting constraints on the temperature of the Långban fissure assemblages. Studies of strontium and common lead isotope systematics in the Långban-type deposits were made by Åberg & Charalampides (1986, 1988), who concluded that, on the basis of common lead data, mineral formation at Långban took place within a restricted time-interval. As is the case with several other deposits in Bergslagen, no reasonable model age could be achieved.

Closure and flooding of the mines since the early 1970s make the deposit inaccessible. Hence this study is based on specimen material from the collections of the Swedish Museum of Natural History (SMNH), Stockholm. Some of the older specimens are precisely located within the mines (Table 1). Furthermore, field work in the greater Långban area was conducted in order to investigate the presence of similar mineralized assemblages on a larger scale.

Geological Setting

The Långban deposit (59.86°N, 14.27°E) is situated in the westernmost part of the Paleoproterozoic Bergslagen ore province, southwestern central Sweden (Fig. 1). The geology of Långban and the surrounding area has been previously studied by Magnusson (1930), Björk (1986) and, to some extent, Lundström (1995). Långban thus belongs to the economically important Bergslagen ore province, which comprises most of the Southern volcanic belt of the *ca.* 1.9–1.8 billion years old Svecokarelian province (*e.g.*, Lundström 1999). Bergslagen is characterized by metavolcanic rocks, including rhyolitic pyroclastic caldera formations and dacitic–rhyolitic complexes (Allen *et al.* 1996), overlain by metasedimentary rocks. The sequence of supracrustal rocks has been intruded by several generations of granitic rocks. It is in part strongly deformed and generally metamorphosed to upper greenschist and amphibolite facies, of which the latter predominates. Most of the mineralization occurs in the upper part of the metavolcanic sequence and is considered to have formed in a relatively shallow subaqueous environment as felsic volcanism waned (Allen *et al.* 1996). The formation of the primary oxide ores has been subject of debate (*e.g.*, Sjögren 1910, Magnusson 1930). A general study of the primary oxide mineralization, including

TABLE 1. SAMPLES, MINERAL ASSEMBLAGES AND FLUID-INCLUSION (FI) DATA, LÅNGBAN DEPOSIT, BERGSLAGEN, SWEDEN

Sample no. (location*)	FI host mineral (s)	Associated minerals	Fissure host **	FI data
SMNH 30806	barite	Nad, Ins, Cal	phyllosilicate	(T_h) boiling conditions; T_m –2 to –10°C
SMNH 883575	calcite	Nad, Arm, Brt	carbonate	T_h 80–180°C; T_m –3.5 to –20°C
SMNH 25506	calcite	Rds	carbonate	T_h 78–110°C
SMNH 12412	barite, calcite	All, Car	tectonized carbonate	Barite: T_m –6.4 to –9.4°C (partly boiling conditions). Calcite: T_h 103–130°C; T_m –7.4 to –11°C
SMNH 13635 (Japan?)	allactite, calcite	Brt, Pb, Pyc, Cu	carbonate	Allactite: T_h 97–120°C; T_m –3 – to –6°C Calcite: T_h 90–140°C; partly boiling conditions, halite present; T_m –1.4 to –30°C
SMNH 500585, 500582 (Japan)	allactite	Brt, Cal	carbonate	T_h 92–120°C; T_m –0.4 to –10°C
SMNH 670497	calcite	All, Brt	carbonate	T_h 78–110°C; T_m –0.4 to –18°C
SMNH 30309	calcite, barite	All, Pyc, Pb	carbonate	Barite: T_h (138–295°C) boiling conditions; halite present. T_m –10 to –24°C. Calcite: transition from boiling to one-phase assoc.; halite present;T_m –3 to –32°C
SMNH 254957	calcite	Nas, Bsl, Pb	tectonized carbonate	T_h 72–140°C; T_m –0.6 to –10°C
EJ 0313–1 (Amerika)	calcite	Nad	hematite ore	T_h 74–115°C; T_m –4.2 to –10.3°C
SMNH 27347 (Collegii)	allactite, barite, calcite	—	silicate-rich carbonate	Allactite: T_h 81–100°C, T_m –7 to –9°C. Barite: (T_h) boiling conditions, T_m –0.5 to –18°C. Calcite: T_h n.d.; T_m –7 to –8.5°C
SMNH 883003 (Irland)	tilasite	Cal, D–H, Hem, Pya	hematite ore	T_h 92–130°C; T_m –6.5 to –16.4°C
SMNH 08451 (Japan?)	barite, tilasite	All, Cal	carbonate	Tilasite: T_h 80°C, T_m –6.5°C. Barite: (T_h) boiling conditions; T_m –1.6 to –11°C
SMNH 35132	sarkinite (euhedral)	Kut	silicate-rich carbonate	T_h 97–115°C; T_m –2 to –5.5°C
SMNH 25163 (Japan–Hindenburg)	sarkinite	Brt, Cal	carbonate	T_h 83–124°C; T_m –8 to –12°C
SMNH 24199 (Japan–Hindenburg)	sarkinite	Brt, Cal	carbonate	T_h 90–110°C; T_m –0.1 to –1.7°C
SMNH 532137	calcite	Pyc, Pb	carbonate	T_h 78–121°C; T_m –9 to –10°C
SMNH 338935	calcite	Car, Lan	carbonate	T_h 150°C; T_m –6.4 to –20.3°C
SMNH 16395	barite	All, Pyc, Pb	carbonate	(T_h) boiling conditions;T_m –3.6 to –8°C

Symbols: All: allactite, Arm: armangite, Brt: barite, Bsl: barysilite, Cal: calcite, Car: caryopilite, Cu: native copper, D–H: dixenite–hematolite, Hem: hematite, Ins: inesite, Kut: kutnohorite, Lan: lanarkite, Nad: nadorite, Nas: nasonite, Pb: native lead, Pya: pyroaurite, Pyc: pyrochroite, Rds: rhodochrosite. * Locations, separate workings within the Långban mines. ** Carbonate rocks are generally Mn oxide-bearing.

geochemistry and genesis in a plate tectonic framework, was presented, by Boström *et al.* (1979), and their synvolcanic submarine-exhalative concept is still generally accepted as the most likely. Furthermore, Bollmark (1999) presented some geochemical data on the host rocks of the mineralized zones, in general supporting the view of Boström *et al.* (1979), as well as suggesting a brief model for the folding of the orebodies. A *ca.* 1.89 Ga submarine-exhalative origin for a majority of the key elements present in the Långban-type deposits was shown to be most likely by Holtstam & Mansfeld (2001), in a mineralogical and geochemical study.

The major ores at Långban consist of syngenetic Fe and Mn oxides, which occur as adjacent, but chemically distinct folded layers within a dolomitic marble. The ores are dominated by an iron-rich type, composed of mainly hematite (± quartz and magnetite), and a manganese-rich type, dominated by braunite and hausmannite. The orebodies have been described in detail by Magnusson (1930) from observations made during mining. The ore-bearing dolomite is situated on top of a thick succession of metamorphosed *ca.* 1.89 Ga rhyolitic volcanic rocks (Fig. 1) having K-rich compositions. Fe and Mn skarn bodies envelop the respective type of oxide ore, and have formed during regional metamorphism and possibly also in conjunction with the early to late orogenic emplacement of granitic magma. The pile of supracrustal rocks is cut by a variety of intrusions, of which the oldest are metabasic, including both doleritic and dioritic types. Granitic plutons, encompassing true granites to dioritic rocks, are abundant in the area and comprise the early Horrsjö granite (1850 Ma; Åberg *et al.* 1983), the late orogenic Hyttsjö granites and diorites (1841 Ma; Oen & Wiklander 1982), and the post-orogenic Filipstad granite (1783 Ma; Jarl & Johansson 1988).

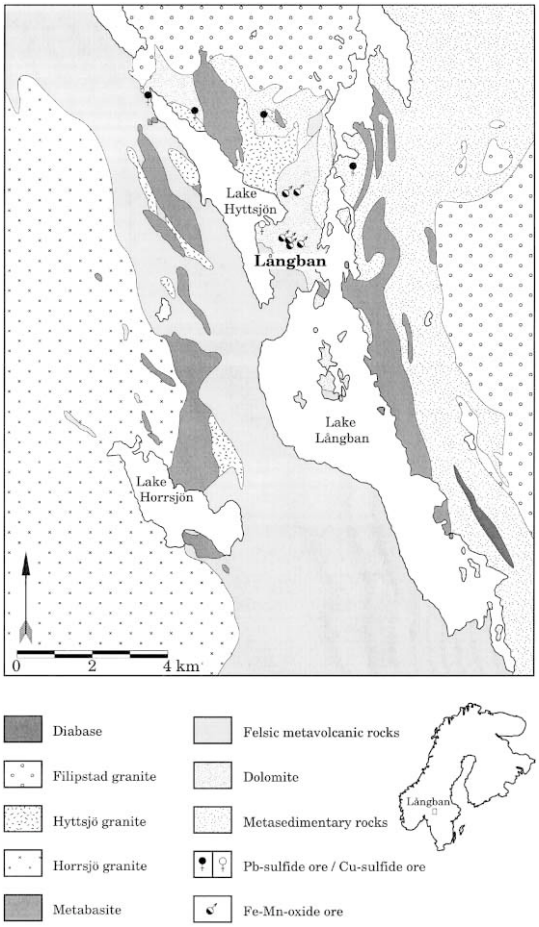

FIG. 1. Simplified geological map of the Långban area (modified after Björk 1986).

Deformation and regional metamorphism associated with the *ca.* 1.85–1.82 Ga Svecokarelian orogeny have affected all older rocks, with peak conditions of metamorphism attaining 550–600°C and 3–4 kilobars in the Långban area (Björk 1986, Lundström 1995, Grew *et al.* 1994, 1996). Retrograde assemblages of minerals imply a post- or late-orogenic event of lower greenschist grade, which is likely to be related to granitic magmatism (Hyttsjö or Filipstad intrusive suites) in the area. Finally, it is obvious from both field studies and specimen-scale textural studies that a later, post-metamorphic, brittle deformation has affected most rocks at Långban. Large-scale lineaments (Björk 1986) as well as partly exposed brittle-ductile and brittle shear and fracture zones are evident in the area. Fieldwork shows that these coincide spatially with the Långban ores. This was also noted during the time of active mining (*e.g.*, Sjögren 1910, Tiberg 1905, 1910, Magnusson 1930). Brittle shear or fracture zones in particular are likely to be related to the channeling of post-metamorphic aqueous fluids responsible for the mobilization of metals and subsequent deposition of fissure assemblages at Långban. A potential cause of these fracture systems may be the *ca.* 1.0 Ga deformation zone of the Sveconorwegian orogeny, which has recently been shown to extend into this area (Wahlgren *et al.* 1994, Page *et al.* 1996).

The fissure mineralization of interest here occurs in rocks dominated by mainly dolomitic marble, Fe and Mn oxide ores, and oxide- and silicate-impregnated carbonate rocks. More rarely, true fissures are found within the Fe and Mn skarn units. During field work, no examples of Pb–Mn–As–Sb-bearing fissure mineralization were observed in the various rocks outside the mine area (Fig. 1), suggesting that the system of mineralized fissures is of a very local nature. Furthermore, typical fissure-assemblages found during mining in the late 1800s and the early 1900s were mainly from the workings in the northwestern part of the mining area (west of the New Shaft, "*Nya Schaktet*"; Flink 1923). There is thus a specific local distribution of this mineralization, as also corroborated by the few and closely located mine workings that supplied typical specimens of fissure assemblages in the museum collection (SMNH) investigated.

PARAGENESIS

A four-stage paragenesis diagram for the Långban ores was presented by Magnusson (1930). Although his diagram is partly an oversimplification and does not take current knowledge about geology and mineral-forming processes into account, it is still useful as a starting point. In Magnusson's first stage, "A", the primary Fe–Mn oxide minerals (or rather, their metamorphic equivalents) were formed together with the earliest skarn minerals. The second stage, "B", represents minerals including skarn assemblages formed during the peak metamorphism of the ores and the marble. The vein and fissure assemblages within the Långban deposit correspond approximately to stages "C" and "D" of the model, respectively, with "C" representing the formation of veins and *Schlieren* assemblages at decreasing temperature, and "D" assigned to the strictly low-temperature brittle fissure-controlled mineralization. The youngest fissure-controlled assemblages are, in addition to the ubiquitous barite and calcite, characterized by the occurrence of native metals, Pb oxychlorides, hydroxylated arsenates, arsenites, and Mn oxides and hydroxides. The fissure minerals generally are euhedral crystals lining partly open cracks. Native lead, pyrochroite, allactite, barite and calcite in various proportions (Sjögren 1886, 1887, Sjögren 1905) typically constitute a late assemblage in the fissures, indi-

cating that the alkaline, reducing conditions needed for its formation were prevalent at that stage.

The Mn content of carbonates increased in successively younger assemblages (Sundius 1963). Arsenate minerals show a trend from the essentially anhydrous early-formed arsenates in stages B–C of Magnusson (1930), to distinctly hydroxylated arsenate species, in particular allactite and sarkinite, during the main part of the D stage. Successively later species, such as manganese-hörnesite, synadelphite and eveite, contain essential H_2O. The paragenetic position of the druses in the iron–manganese skarn is at present debated. The major assemblages are typical of fairly high temperatures (Ketefo 1989), but these are in some cases overgrown by later-formed species more akin to those of the late-stage fissure-type mineralization.

The main focus of this study has been on the most characteristic Mn-arsenate-bearing fissure assemblages. These occur mainly within the dolomitic carbonate rocks, with varying amounts of manganese-bearing silicates (*e.g.*, phyllosilicates) and oxide ore mineral (hausmannite, braunite, jacobsite–magnesioferrite) impregnations. Calcite and barite are ubiquitous in the Ba–Pb–Mn–As–Sb-bearing fissures and are found predating, postdating, as well as coexisting with arsenates, arsenites, oxychlorides, native metals, hydroxides and minor amounts of silicates. A selection of characteristic samples of fissure-type mineralization were singled out for fluid-inclusion studies (Table 1).

Fluid Inclusions

Fluid inclusions were examined in fissure-hosted allactite, barite, blixite, calcite, finnemanite, sarkinite and tilasite. Blixite [$Pb_2Cl(O,OH)_2$] and finnemanite [$Pb_5(As^{3+}O_3)_3Cl$], yielded only very small (<3 μm), possibly primary one-phase inclusions, which could not be further characterized owing to their minute size and dark host mineral (finnemanite). However, their presence is a further indication of a very low temperature of formation for this part of the fissure system, as no bubble formed on cooling of the trapped fluid.

Aqueous fluids dominate fluid inclusions in the samples studied and occur in the form of primary, pseudosecondary and secondary inclusions, as defined by Roedder (1984). Primary inclusions typically occur more isolated, often in crystal cores, possibly related to primary crystal-growth features.

From petrographic investigations, it is evident that repeated fracturing has affected the fissure assemblages. This activity commonly resulted in the occurrence of several types and generations of inclusions present within any given sample. Generally, fluid inclusions in the late-stage, low-temperature minerals are fairly small, many being in the range of *ca.* 2–15 μm. Larger (up to over 150 μm) inclusions may in places have been subject to necking-down. Measurements were not made on these.

Methods

Fluid inclusions were studied in unprepared single crystals and crystal fragments as well as in doubly polished "wafers" approximately 150 μm thick, both of coherent assemblages of fissure minerals and sections of euhedral crystals. As some types of inclusions were investigated in both prepared ("wafers") and unprepared samples (platy crystals), the matter of changes in fluid inclusions during heat-generating and mechanically destructive preparation could be assessed to some degree. No changes were observed, except for the obvious abundant leakage of inclusions situated near the edges and surfaces of sections.

The microthermometric analyses were made on a Chaixmeca heating–freezing stage (Poty *et al.* 1976) mounted on a Leitz microscope utilizing Leitz UMK long working-distance lenses. The thermocouple readings were calibrated by means of Merck melting compounds and SYN FLINC synthetic fluid inclusions. The precision of the measurements was ±0.2°C for ice-melting temperatures and ±1°C for homogenization temperatures.

In order to identify small mineral grains and inclusions in the samples without destroying them, as well as to characterize trapped phases in fluid inclusions, laser Raman microspectrometry was performed utilizing a Dilor XY Raman spectrometer (very similar to the one described by Burke & Lustenhouwer 1987). Exciting radiation was provided by the green line (514.5 nm) of an Innova 70 argon laser. The laser beam was focused through a 100× objective in an Olympus microscope. Calibration was made with respect to wavenumber using a neon laser and a silicon standard.

The identification of mineral species was done with standard powder X-ray-diffraction technique (Philips PW 1710 diffractometer utilizing Cu*K*α radiation), supplemented by semiquantitative SEM–EDS analysis (Philips SEM 515, EDAX 9800 system) and, in a few cases, electron-microprobe analysis (wavelength-dispersion spectrometry; Cameca SX–50).

Fluid inclusions in calcite and barite

Fluid inclusions were studied in several assemblages of calcite and barite. A rough chronological division of different populations of fluid inclusions has been made based on their spatial appearance in the crystals and their temporal relation to recognized episodes of boiling.

In some early coarse and sparry calcite, fluid inclusions representing a preboiling stage may be present. These, as well as later calcite-hosted fluid inclusions from in-between boiling episodes in the main fissure, consist of two-phase (liquid + vapor) inclusions that have a primary or pseudosecondary occurrence at random or in clusters. They commonly have a negative rhombohedral shape, in some cases grading into elongate tubular to round shapes within the same clus-

ter. The degree of fill is generally more than 0.9, with size varying between 2 and 20 μm. A subtype of these has a more angular shape and slightly larger size, up to 50 μm. Many inclusions of this subtype exhibit evidence of necking-down. Secondary one-phase (liquid) inclusions in the same samples are arranged along healed planar fractures. These inclusions are elongate, roundish or tubular, with lengths up to 50 μm.

In a later generation of calcite, which occurs as well-developed scalenohedra, and in late barite, fluid inclusions that represent the syn- and post-boiling stages are present. Primary "syn-boiling" inclusions (Fig. 2) occur at random or as clusters in barite and the cloudy base of calcite scalenohedra. Coeval inclusions have varying proportions of phases, from inclusions that are filled with a liquid, to inclusions with different vapor-to-liquid ratio, to inclusions completely filled with a vapor phase. In some inclusions, generally elongate roundish and up to *ca.* 50 μm in size, with a degree of filling of <0.6, a solid mineral phase may be observed (Fig. 3a). It exhibits a generally well-developed cubic form, and is translucent and isotropic. Laser Raman investigations gave no detectable signal. All these distinctive features, together with its behavior upon heating (see below), suggest the presence of halite.

Two different populations of "post-boiling" inclusions are distinguished in late calcite and barite. Primary inclusions in calcite are dominated by two phases (liquid and vapor), and they have similar shape and size as the "pre-boiling" primary inclusions.

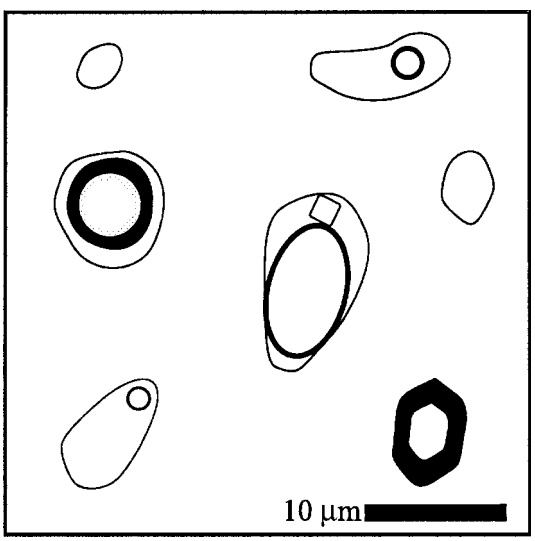

FIG. 2. Sketch of a typical assemblage of fluid inclusions representative of boiling conditions in the Långban fissures; one-phase inclusions (liquid or vapor only), two-phase inclusions (liquid + vapor in different ratios), and three-phase inclusions (liquid + vapor + halite).

Primary one-phase (liquid) inclusions occur relatively isolated without preferred orientation both in calcite and barite (Fig. 3b). The inclusions are elongate, roundish to angular, in some cases "faceted" in morphology. Their size generally is between *ca.* 10 and 50 μm.

Fluid inclusions in allactite

The hydroxyl-bearing manganese arsenate allactite [$Mn_7(AsO_4)_2(OH)_8$] is one of the most characteristic "exotic" fissure species at Långban (*e.g.,* Aminoff 1921). It is generally found as subhedral to euhedral crystals associated with, or included in, calcite, barite, native lead and pyrochroite [$Mn(OH)_2$]. Fluid inclusions were studied in three types of allactite. The best-suited allactite consists of isolated, platy crystals; their general transparency and platy habit made it possible to use them directly for measurements in the heating–freezing stage. Other paragenetic types of allactite, especially larger, partly intergrown crystals, as well as smaller subhedral and completely intergrown individuals, could not be handled in this way and were prepared as doubly polished "wafers".

Of those allactite crystals that contained suitable inclusions, both primary and secondary populations have been identified. Primary inclusions consist of two phases (liquid + vapor) and have a random occurrence and random to subparallel orientation (Fig. 3c). Their shape is angular to round in cross-section, and elongate and tapering, with sizes between 10 and 90 μm. The degree of fill is typically >0.9. The larger of these inclusions are commonly more-or-less reticulated owing to necking-down and similar post-trapping processes. Secondary or pseudosecondary two-phase (liquid + vapor) and one-phase (liquid) inclusions are present in small clusters and linear or planar arrangements. The shape of the inclusions is round to slightly angular. Their size is 3–20 μm, and the degree of filling is greater than 0.9.

Another population of secondary inclusions occurs along fractures and possible cleavages in large and coarse crystals of allactite included in pyrochroite, together with minor native lead, hydrocerussite, calcite and barite. However, the morphology, exposed position and variable proportions of phases (liquid + vapor) suggest that these inclusions have suffered from extensive leakage and other post-trapping alteration (coeval with precipitation of pyrochroite). Darker and less translucent, intergrown subhedral crystals of allactite in this assemblage contain few small groups of two-phase fluid inclusions, which probably are of secondary origin.

Fluid inclusions in sarkinite

Sarkinite [$Mn_2(AsO_4)(OH)$] mainly occurs in fissures hosted by a hausmannite-bearing dolomitic carbonate rock (*e.g.,* Flink 1924). Both primary and

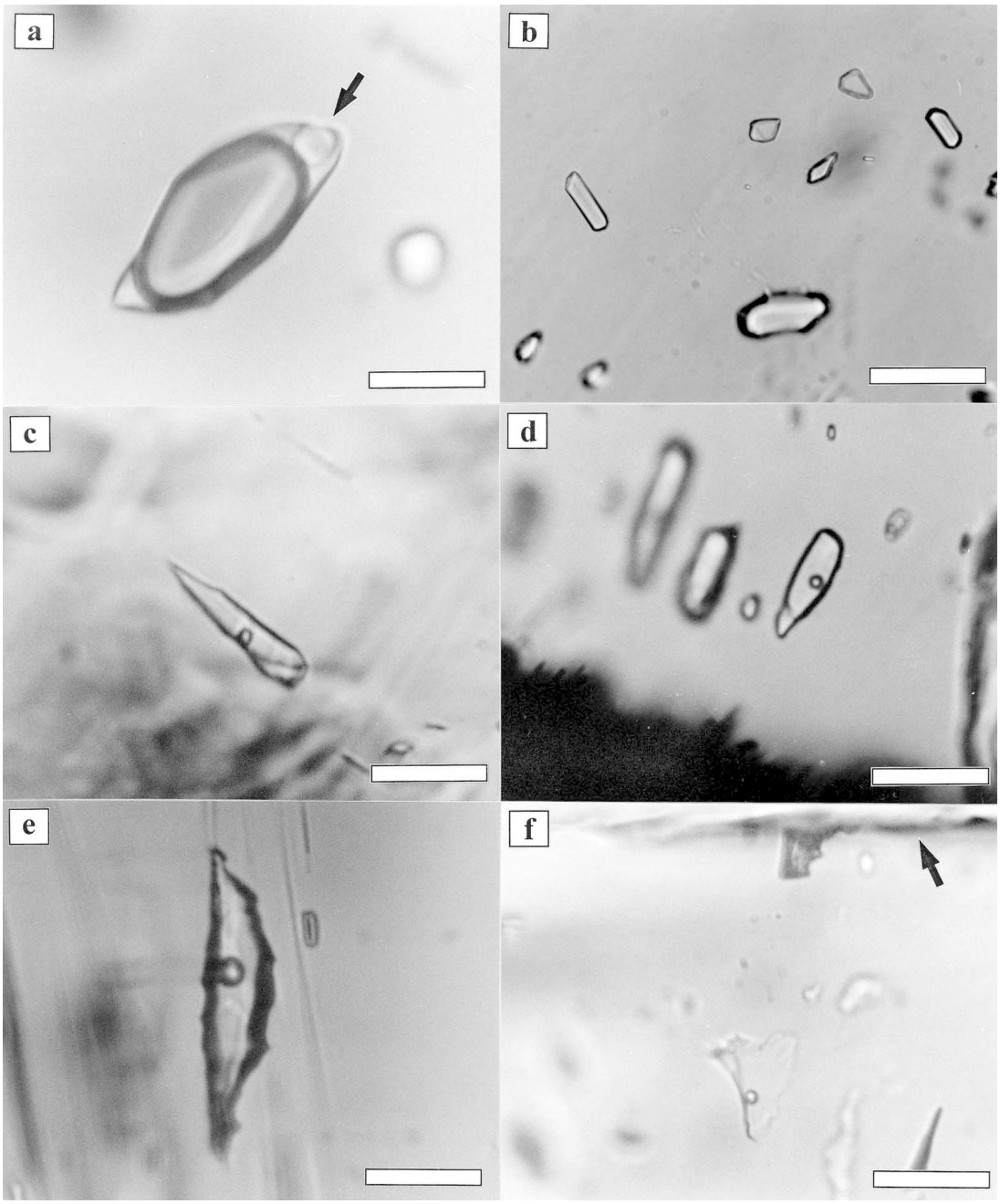

FIG. 3. Photomicrographs of fluid inclusions. (a) Halite-bearing (arrow) vapor-rich inclusion from boiling assemblage in barite. Scale bar equals 15 μm. (b) One-phase aqueous fluid inclusions in upper part of scalenohedral calcite crystal. Scale bar equals 15 μm. (c) Isolated two-phase fluid inclusion in euhedral allactite. Scale bar equals 15 μm. (d) Two-phase fluid inclusions directly related to earlier growth of Mn silicate (dark, bottom of photo) in sarkinite. Scale bar equals 15 μm. (e) Two-phase fluid inclusion occurring along primary growth-features in sarkinite. Scale bar equals 10 μm. (f) Two-phase fluid inclusion occurring along growth zone (arrow) in euhedral tilasite. Scale bar equals 15 μm. Photos taken in plane-polarized light.

secondary fluid inclusions are present in the massive and in the euhedral types of sarkinite. The primary inclusions consist of two phases (vapor + liquid) with a degree of fill that is invariably close to 0.9. They commonly occur related to primary growth-features, including earlier-formed minerals (Fig. 3d). For the main part, these inclusions occur as clusters and are slightly elongate, subangular but more commonly round, and in some cases tabular. Some have a stepped or jagged appearance (Fig. 3e), or a tendency toward negative-crystal shape. Their size may be up to 40 μm, but is generally below 20 μm. One sample investigated contained, apart from vapor and liquid, sporadic inclusions containing crystals with a distinctly corroded appearance. The unsystematic occurrence implies that the mineral represents an accidental inclusion, rather than daughter crystals. Despite repeated attempts to utilize the laser Raman probe, no positive identification could be made.

Secondary fluid inclusions occur as sheets of coeval one-phase (liquid) and two-phase (vapor + liquid) inclusions along healed microfractures in sarkinite. The vapor phase of the two-phase inclusions is very small, and the degree of fill is more than 0.9. The inclusions are round or subangular and stepped in morphology. Sizes vary between 10 and 100 μm.

Fluid inclusions in tilasite

Tilasite [$CaMg(AsO_4)F$] is a relatively rare mineral in the late fissures, and is found only as euhedral crystals in more or less open fissures and cavities. They generally contain few fluid inclusions. Two-phase (liquid + vapor) inclusions in euhedral tilasite (Fig. 3f) are equant to slightly elongate, with a round to angular and, in some cases, irregular shape. Their size may be up to 20 μm, and the degree of fill exceeds 0.9. The inclusions occur isolated or related to zones of growth within the crystals. Some of the inclusions show evidence of necking-down, but as the degree of fill is consistent (>0.9) throughout any group within a single crystal, these may be used for microthermometry. Necking-down probably took place directly after trapping before the temperature decreased, and while the fluid was still homogeneous, prior to nucleation of the vapor and cooling.

Results of Microthermometry

In many cases, the gas bubble originally present in the inclusion would not renucleate after heating or freezing runs. In particular, some calcite-hosted inclusions, but also many inclusions in allactite, behaved in this way. This may be due to the effect of "high negative pressure" described by Roedder (1984). Thus, it has been difficult to gather complete sets of data from many inclusions (including both homogenization and ice-melting data). However, through the observation of many reversals, and overall petrographic relations, it was possible to inter-relate the inclusions and their characteristics in a meaningful way.

The fact that a large number of inclusions are one-phase and liquid-filled presented an additional problem. For these inclusions, a liquid–vapor homogenization is not possible, and it is therefore generally assumed that such inclusions have been trapped at temperatures below *ca.* 70°C (Roedder 1984). This inference is also corroborated by the lowest measured T_h in this system, ranging between *ca.* 70 and 74°C (Figs. 4a–d). During freezing, the absence of a vapor phase in liquid-filled inclusions may cause metastable melting of ice, which complicates the estimation of the salinity. In such inclusions, it may also be difficult to distinguish ice on cooling and to observe the exact temperatures of phase changes. To avoid metastable melting and to make more exact observation of the freezing characteristics possible, some samples were heated to >200°C in order to stretch the inclusions. This treatment resulted in the development

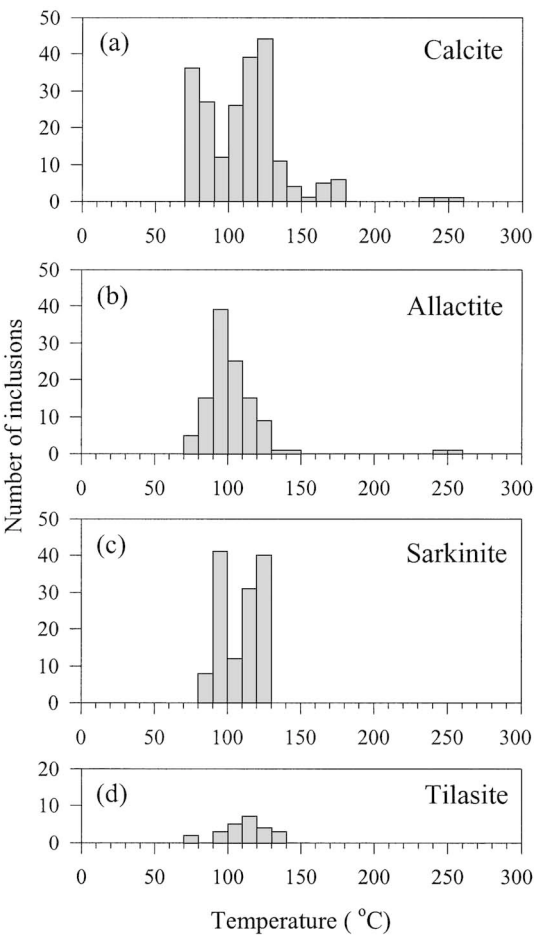

of an "artificial" shrinkage bubble. After freezing the inclusions, all ice-melting temperatures could be measured in the presence of a vapor phase in addition to the liquid. Analyses on inclusions before and after this treatment revealed no significant deviations in measured freezing–melting characteristics, and it is assumed that the possibility of differentiation of the salts in the inclusion fluid is very small and thus negligible immediately after heating.

Compositional variation in the fluid inclusions can be monitored in two different ways through microthermometry: changes in general content of dissolved salts and compositional variations of those salts. The first-observed melting during warming, in the region –70 to –50°C, is an important clue to the composition of the fluid inclusion, but it is generally difficult to observe and interpret unambiguously. In the lower temperature part of this range, such textural changes may also possibly be confused with recrystallization phenomena. The aqueous fluid inclusions in the

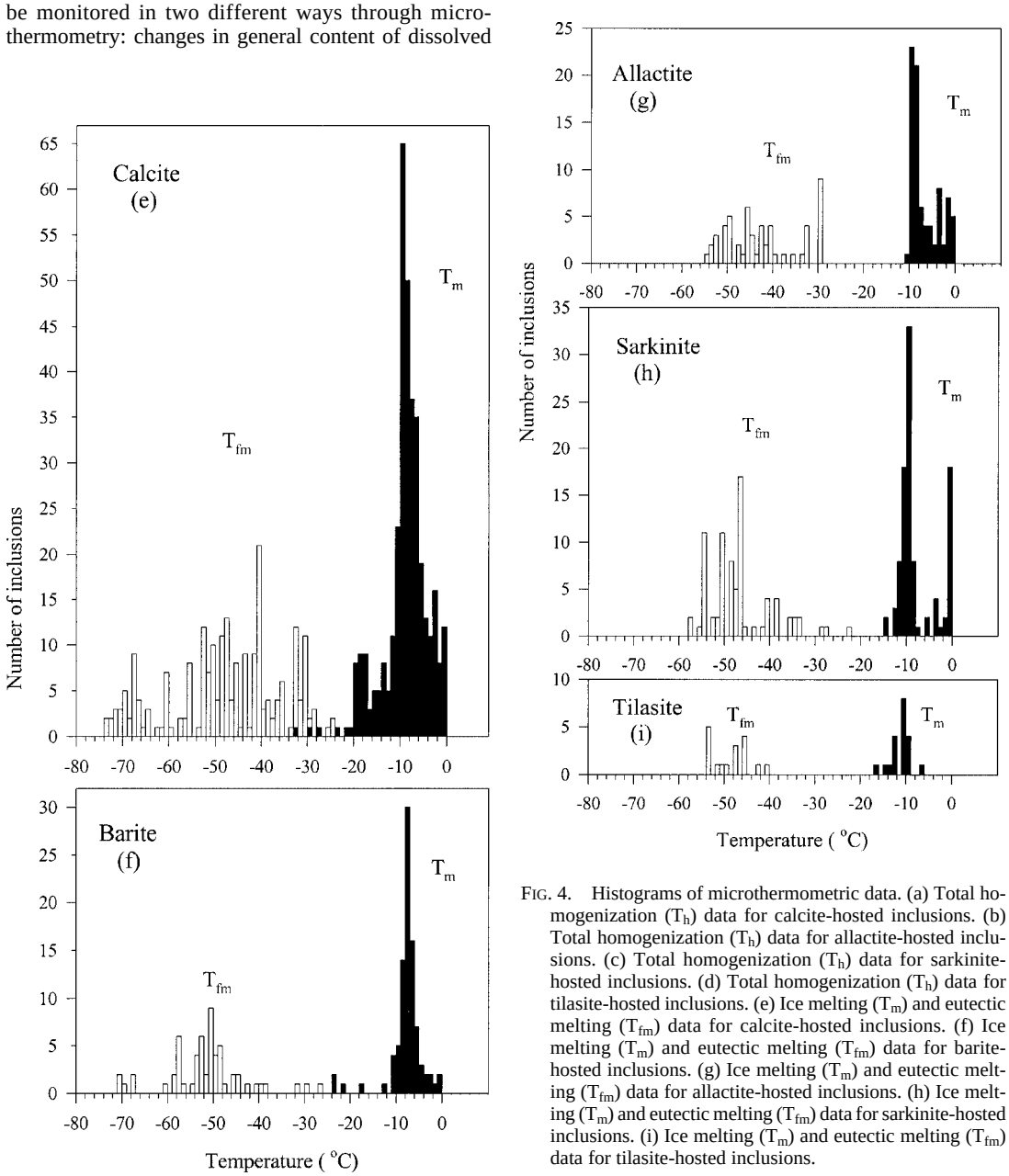

FIG. 4. Histograms of microthermometric data. (a) Total homogenization (T_h) data for calcite-hosted inclusions. (b) Total homogenization (T_h) data for allactite-hosted inclusions. (c) Total homogenization (T_h) data for sarkinite-hosted inclusions. (d) Total homogenization (T_h) data for tilasite-hosted inclusions. (e) Ice melting (T_m) and eutectic melting (T_{fm}) data for calcite-hosted inclusions. (f) Ice melting (T_m) and eutectic melting (T_{fm}) data for barite-hosted inclusions. (g) Ice melting (T_m) and eutectic melting (T_{fm}) data for allactite-hosted inclusions. (h) Ice melting (T_m) and eutectic melting (T_{fm}) data for sarkinite-hosted inclusions. (i) Ice melting (T_m) and eutectic melting (T_{fm}) data for tilasite-hosted inclusions.

Långban fissure system do exhibit abundant low-T melting and recrystallization, as well as higher-T recrystallization features, in the region of –40 to –30°C; these are attributed to a significant $CaCl_2$ component of the dissolved salts, leading to formation of assemblages of ice + hydrohalite + antarcticite on warming (*e.g.*, Davis *et al.* 1990, Walker & Samson 1998, Samson & Walker 2000). An approximation based on these observations suggest $CaCl_2/(CaCl_2 + NaCl)$ values of 0.8–0.9 (Crawford 1981, Shepherd *et al.* 1985). Thus the salinities of this system are expressed as equivalent weight percent ($NaCl + CaCl_2$) and converted from temperatures of final melting of ice (T_m) using the data of $CaCl_2$-rich compositions from Oakes *et al.* (1990). The microthermometric data are presented in Figures 4a–i and Table 1, and summarized in Figures 5 and 6.

Calcite- and barite-hosted inclusions

The homogenization temperatures (T_h to liquid) of primary and pseudosecondary two-phase inclusions in the early calcite and barite range between 70° and 180°C (Fig. 4a). It was not possible to discern any differences or trends between their T_h and the shape of the inclusions.

The varying phase-ratios of coeval primary fluid inclusions representing the "syn-boiling" stage (Fig. 2) are consistent with heterogeneous trapping under conditions of boiling. If the lowest temperature of homogenization of the most liquid-rich and that of the most vapor-rich inclusions in such a population are similar, this value represents the temperature of trapping (Bodnar *et al.* 1985). Measurements of T_h of inclusions with phase ratios between these end-members will result in erroneously high and scattered values, since they have trapped mixtures of steam bubbles and liquid. In the Långban samples, the most liquid-rich inclusions are liquid-only, and the temperature conditions during trapping of the boiling fluid at Långban are best represented by them. Liquid-rich inclusions with a vapor bubble occupying less than 20 vol.% homogenize over a wide range of temperatures, from *ca.* 90° to 256°C. Inclusions with a

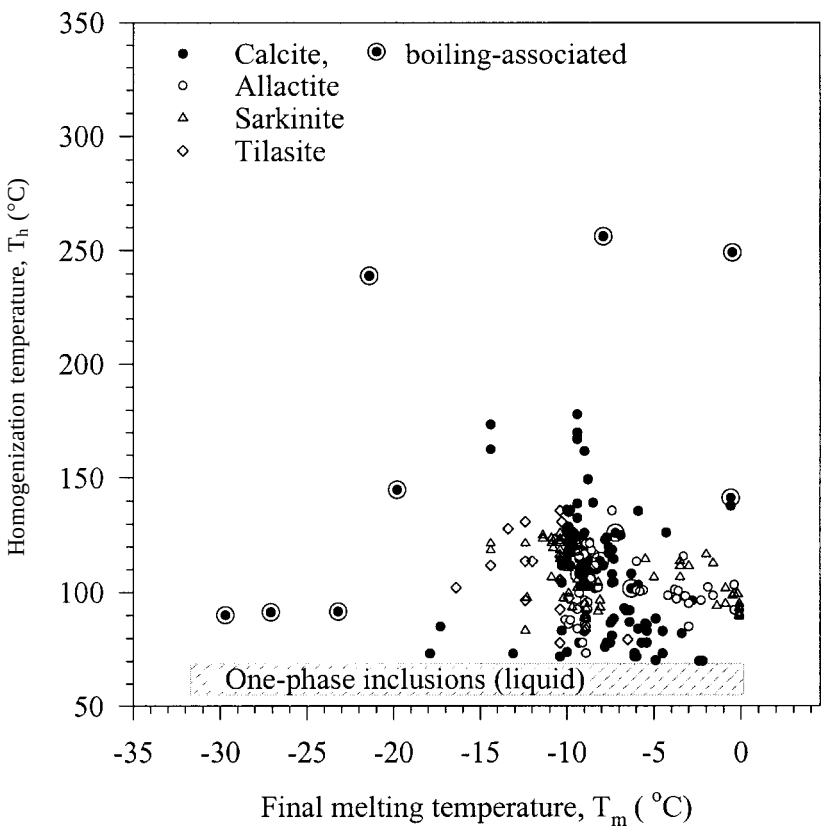

FIG. 5. Plot of homogenization temperatures (T_h, °C) *versus* final ice-melting temperatures (T_m, °C) for fluid inclusions in allactite, calcite, sarkinite and tilasite. The dashed rectangular field indicates the T_m range of one-phase aqueous inclusions.

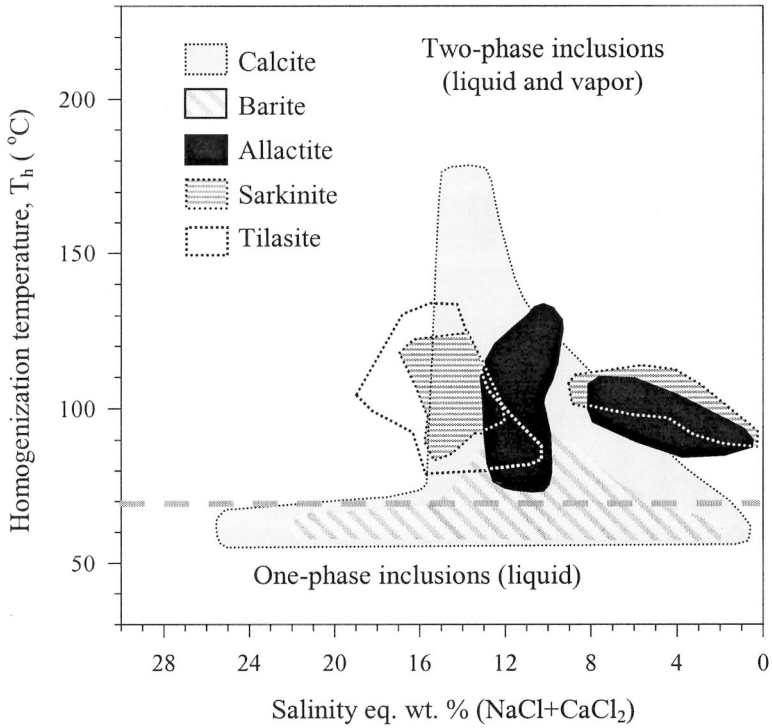

FIG. 6. Summary of temperatures of fluid-inclusion homogenization *versus* salinity data (expressed as eq. wt.% NaCl + $CaCl_2$). Dashed horizontal line at $T_h \approx 70$°C represents the transition from two-phase (liquid + vapor) to one-phase (liquid only) fluid inclusions.

larger vapor phase (20–90 vol.%) commonly decrepitate before a homogenization is achieved (>250°C). Homogenization of the most vapor-rich inclusions is difficult to determine, and the values are considered to be less accurate than for the liquid-rich inclusions.

The majority of homogenization temperatures, T_h, of the two-phase "post-boiling" inclusions range between 75° to 130°C (to liquid). Observed temperatures of first melting, T_{fm}, of all calcite- and barite-hosted inclusions show a large span, from –24° to –71°C (Figs. 4e, f), with most data below –40°C. Typical T_{fm} values for primary inclusions in calcite are –45° to –71°C, and in barite, –50° to –71°C. A similarly large range, *ca.* –30° to –70°C, was measured for secondary inclusions in calcite. The large interval and the low T_{fm} values clearly suggest a range of complex compositions of fluid dominated by NaCl, $CaCl_2$ and possibly $MgCl_2$ (Shepherd *et al.* 1985). The low values of T_{fm} are lower than the eutectic melting reported for salt–H_2O systems including NaCl–$CaCl_2$–KCl–$MgCl_2$ (Crawford 1981, Shepherd *et al.* 1985). However, experimental studies by Davis *et al.* (1990) on melting behavior of fluid inclusions composed of these salt–H_2O systems show that very low values of T_{fm} (down to –80°C) can be ascribed to melting of metastable hydrate phases in solutions containing $CaCl_2 \pm MgCl_2$. The range of T_{fm} is most likely due to variations in the amounts of these salts.

The final melting of ice, T_m, for all fluid inclusions in calcite and barite varies between –0.4°C and –32°C (Figs. 4e, f), which corresponds to salinities in the range 0.5–25 eq. wt.% (NaCl + $CaCl_2$). Fluid inclusions representing the pre-boiling and between-boiling stages typically exhibit salinities around 9 to 15 eq. wt.% (NaCl + $CaCl_2$), whereas the salinities of inclusions trapped during and immediately after the most intense episode of boiling embrace the whole range. The temperature of halite dissolution (above 180°C) is not used for salinity determination because the varying size and phase ratio of the halite cube in individual inclusions, as well as its sporadic presence, indicate that the halite is an accidental phase. Nevertheless, its presence is proof of locally extreme salinities due to boiling, leading to a fluid that in places became supersaturated in NaCl.

Arsenate-hosted inclusions

To our knowledge, allactite, sarkinite and tilasite have never been used before in any study of fluid

inclusions. To ascertain the reliability of the microthermometric data obtained from these minerals, overheating runs were performed. Heating studies show that allactite is not stable above *ca.* 300°C at atmospheric pressure and ambient oxygen fugacity. At this temperature, the interior as well as exterior of the crystals start to darken, presumably owing to rapid oxidation of the abundant Mn^{2+}. Alteration starts along visible microfissures and continues into previously clear and unaffected areas of the mineral. At around 320°C, the crystals become more or less opaque. No apparent leakage, decrepitation or other changes of the fluid inclusions could be observed up to the temperatures at which oxidation sets in. Heating of sarkinite to 400°C does not cause any visible changes to the mineral, but leakage from the largest (>30 μm) inclusions begins at around 200°C, and further heating to 240°C results in decrepitation of all inclusions. Tilasite starts to darken along fractures at *ca.* 380°C, while becoming less transparent. Most fluid inclusions in tilasite decrepitate at around 150°C.

There is no significant difference in microthermometric characteristics between primary, pseudosecondary and secondary two-phase fluid inclusions in allactite; the results are therefore considered together (Figs. 4b, g). Homogenization temperatures, T_h, for all populations of fluid inclusions span a relatively broad interval. The majority display T_h (to liquid) from 74° to 136°C, with a marked accumulation in the range 90–120°C. A few large allactite-hosted two-phase inclusions with a high but variable gas-to-liquid ratio and textures partially evident of necking-down processes exhibited temperatures of homogenization in the range 246–270°C, and some never homogenized before alteration and breakdown of the allactite at 300–320°C. We believe that these inclusions have either undergone extensive leakage or other post-trapping changes in volume, and their homogenization temperatures do not reflect realistic conditions. Observed temperatures of first melting, T_{fm}, occurred from –29° to –54°C. These temperatures are typical of H_2O–Na–Ca–Mg–Cl mixtures (Shepherd *et al.* 1985), and the variation is probably an effect of the $CaCl_2$ quantities in the solution, where the lowest T_{fm} represent $CaCl_2$-rich compositions. The final melting of ice, T_m, shows two distinctive groupings of data, from –0.4°C to –4.4°C and from –5.4°C to –10.1°C. The corresponding salinities of these two groups are 0.5–8 and 9–13 eq. wt.% (NaCl + $CaCl_2$), respectively. These two groups are not present in the same crystals. The highest salinities are in general seen in those inclusions with T_{fm} below –45°C. The presence of two different compositions of salt in the two-phase allactite-hosted inclusions suggests that the active fluids during the formation of the allactite – native lead – pyrochroite – calcite – barite assemblages in the fissures were not allowed to homogenize, but were present as two separate fluid compositions during the relatively short time-span of precipitation of the minerals present.

Sarkinite-hosted fluid inclusions (Figs. 4c, h) have homogenization temperatures (T_h to liquid) between 83 and 126°C, for all types of two-phase inclusions, with a peak at around 90–94°C. Observed temperatures of first melting, T_{fm}, range from –33° to –57°C, with most values below –45°C. These temperatures indicate a H_2O–Na–Ca–Mg–Cl mixture (Shepherd *et al.* 1985). The final melting of ice, T_m, exhibits a grouping from –0.1° to –5.5°C and one from –7.0° to –14.4°C. The T_m data correspond to salinities of 0.2–9 and 11–17 eq. wt.% (NaCl + $CaCl_2$), respectively. The two groups occur in separate crystals from different samples. We found no marked difference between primary and secondary inclusions.

Tilasite-hosted fluid inclusions (Figs. 4d, i) have homogenization temperatures (T_h to liquid) between 80° and 136°C, with a peak around 112°C. Observed temperatures of first melting lie in the interval –40° to –54°C, which points to a H_2O–Na–Ca–Mg–Cl fluid (Shepherd *et al.* 1985). The final melting of ice, T_m, range between –6.5°C and –16.4°C, and correspond to salinities of 10–19 eq. wt.% (NaCl + $CaCl_2$).

Discussion

Fluid-inclusion evidence for boiling within parts of the fissure systems at Långban clearly suggests formation at a minimal lithostatic pressure alternating with open-system behavior at atmospheric pressure for the main part of the arsenate – barite – calcite – native lead – pyrochroite assemblages. Hence, the temperature of trapping (T_t) is assumed to be equal (or very close) to the temperature of homogenization (T_h) for fluid inclusions in the fissure mineralization (Figs. 5, 6). This is also corroborated by estimates of conditions of formation for typical minerals in the fissure (Pb oxychlorides – native elements – hydrated or hydroxylated arsenates – arsenites): these indicate a formation close to, or at, normal atmospheric pressure at very low temperatures. When studying the occurrences of such minerals on a global scale, it is evident that these species form by low-temperature alteration (*e.g.*, by saline marine water) at or very near the surface of the Earth. Many of these species have, except for the Långban-type deposits, only been found elsewhere as superficial products of alteration, exemplified by their formation through seawater – lead slag interaction at Laurion, Greece (*e.g.*, Jaxel & Gelaude 1986, Schnorrer-Köhler 1980). Several assemblages characteristic of the late-stage fissures in the Långban mineralization can be connected with distinct types of occurrences, and thus, distinct processes of formation worldwide. Indeed, the Pb oxychloride minerals comprise a group of chemically and genetically related minerals, which chiefly occur as rare late-stage, low-pressure and low-temperature phases in both marine altered slags and artifacts (*e.g.*, Edwards *et al.* 1992), zones of supergene alteration in base-metal ore deposits (Scott 1994), as well as late-

stage fissure or *Schlieren* assemblages in complex Fe–Mn-oxide ore deposits, such as the Kombat mine, Namibia (Dunn 1991).

It unfortunately is rare to find well-defined constraints on mineral stability useful to evaluate fissure formation at Långban and related deposits, but the presence of domeykite ("α-domeykite" of the older literature) associated with calcite and pyroaurite (± arsenosilicate minerals) in partly open fissures suggests a temperature of formation below 90°C (Burke 1986, Skinner & Luce 1971). This temperature should be compared with the fluid-inclusion data from euhedral prismatic tilasite in a related assemblage (Fig. 4d). These inclusions exhibit homogenization temperatures peaking between *ca.* 90 and 140°C, *i.e.*, only slightly higher than the reported limit of stability of domeykite, and the difference in some tens of degrees may be explained by local variability of temperatures within the fissure system, as domeykite was not observed in the particular specimen used for fluid-inclusion studies.

Parageneses and fluid-inclusion data

In a comparison of the paragenetic sequence with microthermometric data obtained from the host species present, the overall observation is that the system formed in a temperature interval between *ca.* 180°C and well below 70°C, during repeated cracking – boiling – sealing episodes. Subsequent formation of minerals most likely continued for quite some time at temperatures decreasing much below the minimum T_t for the formation of a gas bubble (Roedder 1984).

Fracturing and disturbances of the earlier-formed species also took place during these conditions, as indicated by the apparent secondary nature of cross-cutting planar sets of one-phase inclusions in minerals carrying primary two-phase inclusions. In some specific cases, we suggest that a phase of fracturing and associated formation of secondary two-phase inclusions was almost contemporaneous with the formation of primary inclusions, as such inclusions are similar in gas-to-liquid ratios, salt composition and low temperatures of homogenization. It further is highly likely that the fracturing and subsequent corrosion and healing seen in some assemblages may be due to the violent boiling event, as suggested by inclusions in late barite and calcite.

A correlation between salinity and homogenization data for inclusions in all host minerals investigated (one-phase inclusions, mainly in calcite and barite, are included as the "below 70°C" field; Fig. 6) shows some dramatic changes in the fissure-fluid system at Långban with time. Initially, at temperatures of *ca.* 130–180°C, an intermediate T_m range is seen, representing 9–15 eq. wt.% ($NaCl + CaCl_2$). As homogenization temperatures decrease, a subsequent increase in range is evident in the final melting temperatures and, hence, dissolved salt concentration. At the lower end of the data on homogenization temperature, when passing into the field of one-phase inclusions, concentrations of dissolved salts exhibit a very large range, *ca.* 0.5 to 25 eq. wt.% ($NaCl + CaCl_2$).

Fluid inclusions with varying gas to liquid ratios and without signs of post-formational disruption are consistent with trapping in a boiling fluid system. These fluid inclusions have primarily been observed in barite and, to a lesser extent, in late calcite, both occurring associated with allactite, native lead and pyrochroite. These populations of fluid inclusions are furthermore characterized by the sporadic presence of halite cubes (Fig. 3a). The only inclusions exhibiting halite crystals are those with a relatively high gas-to-liquid ratio (approximately over 40 vol.% gas), thereby suggesting that the process forming these inclusions is closely related to the expulsion of a vapor-rich component during a violent boiling episode where, within the boiling zone, locally steep gradients in salinity may have prevailed. Significantly, halite occurs predominantly in boiling inclusions in barite, which may precipitate very rapidly from an aqueous solution. The commonly radial texture of this barite also implies rapid precipitation (Rimstidt 1997). An earlier generation of subhedral barite also exhibits similar populations of fluid inclusions, but is generally lacking halite. This barite is in turn overgrown by later, sparry calcite carrying primary two-phase (liquid plus gas) fluid inclusions that homogenize in the interval 90–130°C, thereby suggesting a rapid sealing of the fissure system after the first boiling event, and a subsequent increase in temperature with a slight, renewed confining pressure (Fig. 7). Primary fluid inclusions in the basal part of scalenohedral calcite crystals and radial platy barite from a native lead – pyrochroite – allactite assemblage (Fig. 7) vary from an early-formed syn-boiling association consisting of coeval one-phase (gas or liquid), two-phase (gas and liquid in varying proportions) and three-phase (gas, liquid and a halite crystal) inclusions, to clusters of post-boiling single-phase aqueous inclusions in the later-formed part of the crystal. This sequence records an event starting at temperatures just above the boiling point that led to a non-boiling, high-salinity fluid below *ca.* 70–75°C.

That part of the fissure system was quickly resealed is seen in the allactite-hosted two-phase aqueous inclusions in an assemblage comprising coarse radiating aggregates of platy barite, late scalenohedral calcite and, as the last species formed, allactite (Fig. 7). Except for the presence of platy allactite and general absence of pyrochroite and native lead, the assemblage and texture mimic the main type of fissure. The presence of these inclusions in the hydroxylated arsenate, homogenizing at temperatures between *ca.* 90 and 130°C, suggests that some pressure build-up and temperature increase also occurred after the most violent boiling episode. One-phase aqueous inclusions otherwise characterize the continued formation of minerals after the main boiling event within this part of the fracture system (Figs. 7, 8).

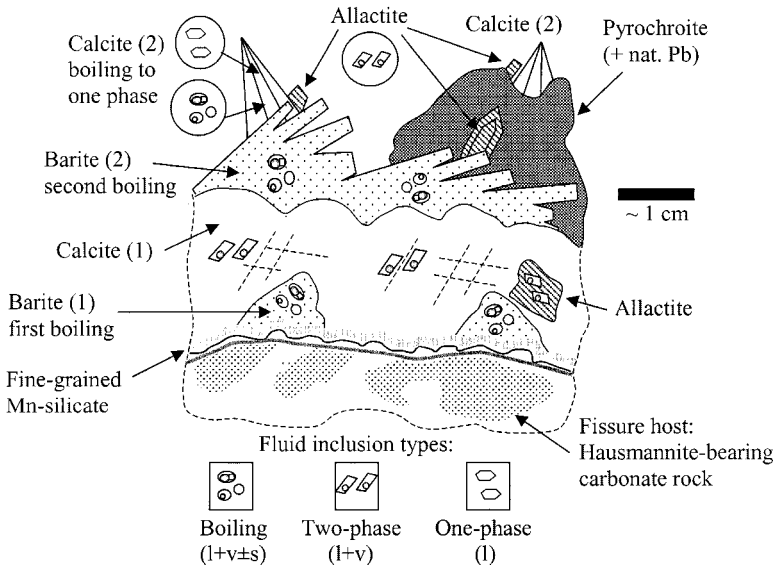

FIG. 7. Schematic diagram for some important fissure-bound species, with indicated evolution of fluid inclusions.

The distinct variation in salinity within petrographically homogeneous populations of inclusions showing evidence of boiling conditions, *e.g.*, in barite and calcite, is considered to result from trapping of a heterogeneous fluid in an active boiling zone (Scott & Watanabe 1998). It is possible that the low-salinity inclusions present in these assemblages may be due to condensation and subsequent trapping of a previously expelled vapor phase. The late introduction of a low-salinity fluid, mixing with the pre-existing higher-salinity fluid, does not seem likely in view of the textural and light stable isotope (C, O, S) evidence available (Jonsson & Boyce 1999).

Lateral and vertical variations within the main fissure system are reflected by variation of fluid-inclusion characteristics in different arsenates and calcite of otherwise similar paragenetic position. The crucial difference is presumably due to their respective position in relation to the zone of boiling, the composition of the host rock of the fissure, and whether or not their immediate surroundings were sealed off from the open-fissure system rapidly after the main boiling event.

That the fracture system opened and (re-)sealed relatively quickly is also manifested both by textural and fluid-inclusion evidence, with the succession of boiling-induced precipitation of barite and subsequent formation of calcite at gradually slightly elevated temperatures with a slight overpressure. Rapid precipitation and coupled sealing of fissures, or parts of the fissure system, may also in part explain the contrasting T_h–salinity trends, as well as diversified paragenetic development, through encapsulation of fluids in different parts, leading to a local evolution in fluid composition and mineralogy.

The occurrence of fluid-inclusion assemblages containing identical and seemingly contemporaneous one-phase and two-phase (gas + liquid) H_2O inclusions, coexisting in clusters or "sheets" (planar or curved planar arrays of fluid inclusions), as is the case with some sarkinite samples, may have different explanations. In many cases, it seems likely, owing to the overall abundance of one-phase inclusions of that specific type, to assume that some post-trapping leakage has occurred and thus led to the gas bubbles in the affected inclusions. In a few cases, *e.g.*, in massive sarkinite, there seems to be a gradation within single sheets of fluid inclusions from one-phase to two-phase inclusions otherwise featuring identical salt compositions. The thermal gradients in at least some of the fissures thus may have been steep enough to form the two types almost contemporaneously, on a millimeter scale. The evidence from several assemblages for a temperature near or slightly above the boiling point of an aqueous fluid, together with a slight confining pressure, supports this concept.

Compositional evolution of fluids

During the introduction of an initially acidic brine bearing metals + S in the fissure system, reaction of the brine with the dolomitic rock dissolved $CaCO_3$ and leached Ba^{2+} and Pb^{2+}. Some lead was most likely al-

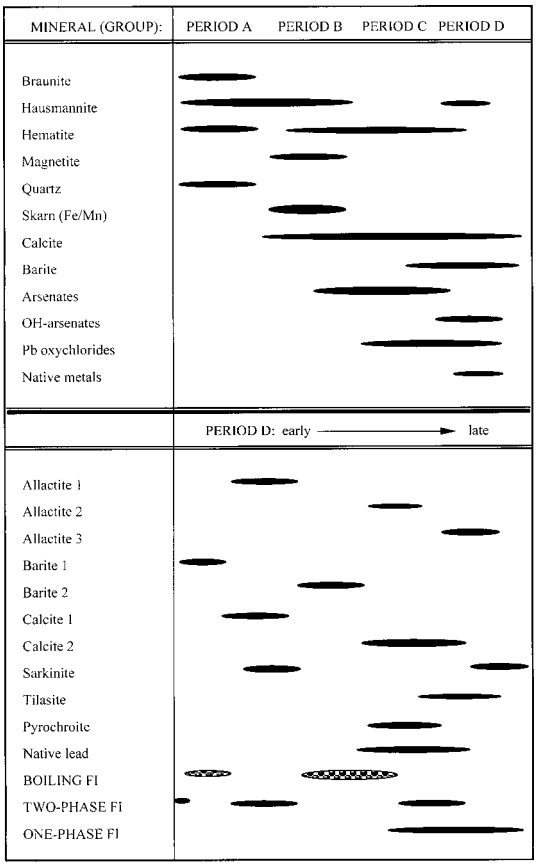

FIG. 8. Paragenesis diagram. Upper box outlines periods A–D of Magnusson (1930); lower box shows important minerals in fissures and fluid evolution during the main stage of the D period. Interpretation is based on observations in "wafers", thin sections, hand specimens and data from Magnusson (1930).

ready present in the fluid, leached together with other metals (*e.g.*, Cu, As) from more deep-seated parts of the volcanic-exhalative mineralization.

At low pH, chloride has been envisaged as an effective complexing agent for lead in many mineralizing solutions, but at higher pH, the stability of such complexes decreases (Seward 1984, Seward & Barnes 1997). Other complexes like $PbHCO_3^+$ or $Pb(HS)_2$ may instead become dominant. At the relatively low temperatures (<200°C) in the fissure systems, $Pb(HS)_2$ is likely to have been the most stable complex present (Reed & Spycher 1985). The transport of As is poorly understood, but according to Webster (1990), $HAs_3S_6^{2-}$ appears to be an important complex at neutral to alkaline conditions. Subsequent interaction of the solution with host rocks bearing hausmannite [Mn_3O_4] leached Mn^{2+} and changed the pH from slightly alkaline to much higher values. Following the discussion by Boström (1965), a likely process for the creation of a strongly alkaline solution can be described by the reaction $HS^- + 4Mn_3O_4 + 11H_2O = 12Mn^{2+} + SO_4^{2-} + 23OH^-$. Because of the very low solubility of $BaSO_4$ (Blount 1977), this reaction, with oxidation of the reduced sulfur to sulfate, and the availability of Ba^{2+} (Boström & Joensuu 1974), resulted in the first generation of barite during boiling conditions (Figs. 7, 8).

The abrupt drop in pressure and consecutive boiling may have had several direct effects on the solution; primarily, it led to massive precipitation of radiating barite due to decreasing solubility of sulfate with decreased pressure (Rimstidt 1997). Secondly, there was an instantaneous concentration of solute in the zone of most extensive boiling, as is seen in the sudden appearance of inclusion-hosted halite crystals and the obvious increase of salinities in contemporaneous and the immediately post-boiling fluid inclusions. The resulting increased salinity in the active boiling zone may eventually have increased the solubility of sulfate (*e.g.*, Blount 1977), but we suggest that at this stage, the effect of instantaneous reduction in pressure is more important than salinity-dependence. The latter is notably also an effect of the pressure-release-induced boiling and coupled decrease in total fluid volume, and thus effective only after the massive precipitation of sulfate had started.

The precipitation of calcite following that of barite may be explained in part by excess carbonate in solution after the sudden precipitation of sulfate, and in part by increasing temperature and subsequent decrease in carbonate solubility. Consequently, the rapid removal of sulfur from the solution led to destabilization and dissociation of the metal complexes. Temperature increased, and calcite was precipitated. Self-sealing of the fractures allowed the pressure to reach a level where boiling declined and finally ceased. At these conditions of high pH, the hydroxylated arsenates became stable, and allactite [$Mn_7(AsO_4)_2(OH)_8$] or sarkinite [$Mn_2(AsO_4)(OH)$] precipitated. Depending on local fluctuations in the amount of Mn^{2+} or As present in the solution as well as pH, the hydroxylated arsenates, or pyrochroite [$Mn(OH)_2$], may have formed. Pyrochroite and native lead were deposited where large amounts of OH^- were produced and an extremely high pH condition was created (Boström 1965); this environment was achieved locally during a second, more violent boiling event. The occurrence of abundant pyrochroite and native lead in fissures hosted by hausmannite-bearing carbonate rocks is evidence that this host-rock played an important part in their formation. The OH-free arsenate tilasite [$CaMg(AsO_4)F$], occurs as a very late species in the fissures bearing allactite – native lead or in open fissures in Fe-oxide-dominated host-rocks, implying formation from fluids relatively depleted in Mn, and with a lower pH.

Sources of fluids and metals

In previous studies of Långban and the surrounding area (*e.g.*, Moore 1970, Björk 1986), late orogenic intrusions such as the Hyttsjö suite were suggested to have acted as an external source of metals for the Långban system. However, minerals containing essential granite-derived elements, such as B, Be, F, Mo and Sn, are very limited in the late mineralized fissures. Species carrying these elements are concentrated in assemblages belonging to stages B–C of Magnusson's (1930) paragenetic sequence (Fig. 8). The only known examples of such species occurring as fissure minerals are the very rare Be minerals aminoffite and barylite, and the Sn minerals wickmanite and tetrawickmanite. Tilasite and fluorite are also present as rare species in the fissures, albeit they are more common than the ones just mentioned. No evidence has been found of any larger-scale remobilization or introduction of granite-associated elements during the youngest (D) stage. Thus, any influx of granite-derived, fractionated fluids probably did not occur during the stage of true fissure-confined mineralization, but may have taken place during an earlier event, presumably at significantly higher temperatures. Furthermore, the fact that all known systems of brittle fissures outside the principal Långban mine area have been found to be barren of Pb–Mn–As–Sb mineralization indicates that the systems were very local in nature, and thus the most likely source of metals is the pre-existing *ca.* 1.89 Ga carbonate-hosted volcanic-exhalative deposit.

Whereas it seems unlikely that any notable amounts of metals were introduced from external sources during the fissure-forming phase, the situation with chlorine is different; this component may have been introduced on a larger scale through circulation of a marine or magmatic water, or a water with a significant component of one of these. The ubiquitous presence of chlorine is seen in microthermometric data, as well as through the abundance of Cl-bearing minerals present in the fissures. Contributions of salt from meta-evaporites within the surrounding pile of supracrustal rocks to an infiltrating meteoric water may also be advocated, but the lack of evidence for the presence of true meta-evaporite horizons in this part of the Bergslagen district makes that option less likely. Boström *et al.* (1979) did suggest that the initial Fe–Mn oxide ores were deposited by submarine-exhalative processes involving a hot brine; this then saturated the original deposits with salts like NaCl, which may have been available for later remobilization. Thus, a later, deep convecting, originally low-salinity fluid may have been modified through interaction with host rocks and ores without the need for a separate evaporite horizon. The fluid would then increase in salinity and leach the present metals from the pre-existing volcanic-exhalative ore deposit, and precipitate the resulting minerals in a shallow system of brittle fractures in the upper parts of the deposit. The fact that $CaCl_2$ is an important component of the dissolved salt content in fissure-hosted fluid inclusions further suggests that interaction with the dolomitic carbonate host-rocks may account for a significant portion of the Ca in the fluids circulating along the fissures.

Preliminary carbon and oxygen isotopic studies of vein and fissure assemblages from the Långban deposit (Jonsson & Boyce 1999) failed to show any drastic shift from higher P–T vein assemblages to the low P–T fissures. This finding suggests an intimate relation and interaction between fissure-mineralizing fluids and the pre-existing ores and host rocks.

Formation of fissure minerals in a geological framework

The microthermometric data in this study contradict earlier estimates for a higher-temperature formation of the Långban vein and fissure assemblages. On the basis of sulfur isotope data, Boström (1981, 1996) had suggested initial temperatures of *ca.* 630°C for the deposition of early barite and sulfides, and around 325°C for the formation of native lead – pyrochroite vein assemblages.

Previous investigators suggested that mineral formation at Långban was a continuous process from the time of regional medium-grade metamorphism to mineralization of fractures; this would mean fissure formation at comparatively high pressures and temperatures, which is inconsistent with the fluid-inclusion evidence. In general, mineralogical and paragenetic studies and the available range of mineral stabilities support the present range in homogenization temperatures as being identical with, or very close to, the actual temperatures of formation for the Långban fissure systems. In order to prevent boiling (by a lithostatic or hydrostatic pressure regime), the inferred maximum depth of formation of the barite – calcite – arsenate – native lead – pyrochroite assemblages would be only a couple of hundred meters at most. Gradations in fluid-inclusion types within single fissures suggest that thermal gradients have been significant. Texturally, the brittle-tectonic fissures cross-cut all earlier metamorphic fabrics in the various host-rocks, thus also separating them from earlier, partly plastically deformed veins carrying species typical of a formation at higher pressure and temperature. Only spatially restricted reaction and replacement zones of the fissure matrices can be observed, which also suggests a low initial temperature, a comparatively cool host-rock for the fissures, and the relatively quick cooling and deposition of fissure assemblages.

Thus we contend that the fluids were introduced in a brittle-tectonic fracture setting, post-metamorphic in relation to the *ca.* 1.85–1.82 Ga Svecokarelian orogeny, and focused in a relatively restricted volume of rock. The exact timing of the fissure mineralization cannot be specified at present. Nevertheless, it is likely that the apparent brittle-tectonic setting, coupled with the obvi-

ous need for a thermal event in order to both initiate fluid flow, and subsequently leach metals and redistribute them in the form of a low-P–T assemblage like the Långban system, point toward the locally abundant post-orogenic intrusions of granite (the *ca.* 1.78 Ga Filipstad suite) or possibly the deformational front of the *ca.* 1.0 Ga Sveconorwegian orogeny.

Summary

The major part of the exotic fissure-related mineralization at Långban formed at temperatures between a maximum of *ca.* 180°C down to well below 70°C, from moderately to highly saline $CaCl_2$–NaCl-rich aqueous fluids, through a sequence of boiling events in a near-surface brittle-tectonic environment. This reconstruction stands in clear contrast to previous hypotheses regarding both prevalent P–T conditions, relations to previous geological events, and timing of mineralization.

Initial formation of fissures and subsequent boiling events were triggered by a polyphase late-tectonic event leading to sporadic open-system behavior through repeated release of pressure. Reactions between the fluid and the abundant hausmannite-bearing carbonate host-rock led to modification of the fluid. A drastic increase in pH and a concomitant release of sulfate and Mn^{2+} occurred. Opening of the fissure system led to a resulting drop in pressure, boiling of the fluid, and subsequent rapid precipitation of barite and associated species.

Mineralogical variations within the fissure system reflect lateral variations with respect to the boiling zone, and variations in the substrate of the fissures. The latter governed paragenetic variations through reactions with the initial fluid. The importance of host-rock composition is best exemplified by the predominance of hausmannite-bearing carbonate rocks as substrates for allactite – native lead – pyrochroite assemblages. The hausmannite – carbonate rocks are the only suitable host-rocks to develop the necessary pH conditions in the fluid for the formation of this extreme assemblage.

The metals present in the fissure system are likely to have been derived locally, from the pre-existing *ca.* 1.89 Ga submarine volcanic-exhalative mineralization. Other brittle-tectonic fissure systems outside the Långban mine area are all barren of Pb–Mn–As–Sb mineralization. The tectonothermal episode responsible for this mineralization may well have been the *ca.* 1 Ga Sveconorwegian orogeny or post-Svecokarelian felsic magmatism.

Acknowledgements

We thank U. Hålenius and D. Holtstam, SMNH, as well as K. Boström, Stockholm University, for comments on an early draft of this paper. We are also grateful for the comments and constructive criticism by D. Kontak and D. Marshall (referees) and R.F. Martin, which significantly improved the manuscript. K. Högdahl, SMNH, is thanked for assistance with illustrations; J. Söderhielm, Stockholm, is thanked for his courageous work on preparing "wafers" from the fragile Långban fissure minerals, as is K. Helge, Hunnebostrand. This study was financed by the Swedish Natural Science Foundation (NFR; now *Vetenskapsrådet*) as part of a larger project on mineralization at Långban.

References

Åberg, G., Bollmark, B., Björk, L. & Wiklander, U. (1983): Radiometric dating of the Horrsjö granite, south central Sweden. *Geol. Fören. Stockholm Förh.* **105**, 78-81.

_____ & Charalampides, G. (1986): New lead isotope data from the Långban mineralization, central Sweden. *Geol. Fören. Stockholm Förh.* **108**, 243-250.

_____ & _____ (1988): Evolution of the mineral deposits from Långban, Sweden, as recorded from strontium isotope data. *Geol. Fören. Stockholm Förh.* **110**, 329-334.

Allen, R.L., Lundström, I., Ripa, M., Simeonov, A. & Christofferson, H. (1996): Facies analysis of a 1.9 Ga, continental margin, back-arc, felsic caldera province with diverse Zn–Pb–Ag–(Cu–Au) sulfide and Fe oxide deposits, Bergslagen region, Sweden. *Econ. Geol.* **91**, 979-1008.

Aminoff, G. (1918a): Kristallographische Studien an Calcit und Baryt von Långbanshyttan. *Geol. Fören. Stockholm Förh.* **40**, 273-446.

_____ (1918b): Några iakttagelser angående mineralens paragenes och succession vid Långbanshyttan. *Geol. Fören. Stockholm Förh.* **40**, 535-546.

_____ (1921): Über das Mineral Allaktit. *Geol. Fören. Stockholm Förh.* **43**, 24-52.

Björk, L. (1986). Beskrivning till berggrundskartan Filipstad NV. *Sver. Geol. Unders. ser. Af* **147**.

Blount, C.W. (1977): Barite solubilities and thermodynamic quantities up to 300°C and 1400 bars. *Am. Mineral.* **62**, 942-957.

Bodnar, R.J., Reynolds, T.J. & Kuehn, C.A. (1985): Fluid-inclusion systematics in epithermal systems. *In* Geology and Geochemistry of Epithermal Systems (B.R. Berger & P.M. Bethke, eds.). *Rev. Econ. Geol.* **2**, 73-97.

Bollmark, B. (1999): Some aspects of the origin of the deposit. *In* Långban: the Mines, their Minerals, Geology and Explorers (D. Holtstam & J. Langhof, eds.). Raster Förlag, Stockholm, Sweden (43-49).

Boström, K. (1965): Some aspects of the analysis of mineral forming conditions. *Ark. Mineral. Geol.* **3**, 545-572.

_____ (1967): Some pH-controlling redox reactions in natural waters. *Adv. in Chem., Ser.* **67**, 286-311.

_____ (1981): On the origin of the native lead – pyrochroite association in Långban. *Geol. Fören. Stockholm Förh.* **103**, 120-121.

_____ (1996): The temperature of formation of the native lead – pyrochroite veins and related associations in Långban. *GFF* **118**, A50.

_____ & JOENSUU, O. (1974): Distribution of Ba and Pb in primary carbonates in Långban, Sweden. *Geol. Fören. Stockholm Förh.* **96**, 375-379.

_____, RYDELL, H. & JOENSUU, O. (1979): Långban – an exhalative sedimentary deposit? *Econ. Geol.* **74**, 1002-1011.

BURKE, E.A.J. (1986): Koutekite and some other opaque minerals new for Långban, Sweden. *Neues Jahrb. Mineral., Monatsh.*, 59-64.

_____ & LUSTENHOUWER, W.J. (1987): The application of a multichannel laser Raman microprobe (Microdil-28) to the analysis of fluid inclusions. *Chem. Geol.* **61**, 11-17.

CRAWFORD, M.L. (1981): Phase equilibria in aqueous fluid inclusions. *In* Fluid Inclusions – Applications to Petrology (L.S. Hollister & M.L. Crawford, eds.). *Mineral. Assoc. Can., Short Course Handbook* **6**, 75-100.

DAVIS, D.W., LOWENSTEIN, T.K. & SPENCER, R.J. (1990): Melting behaviour of fluid inclusions in laboratory-grown halite crystals in the systems NaCl–H_2O, NaCl–KCl–H_2O, NaCl–$MgCl_2$–H_2O, and NaCl–$CaCl_2$–H_2O. *Geochim. Cosmochim. Acta* **54**, 591-601.

DUNN, P.J. (1991): Rare minerals of the Kombat mine, Namibia. *Mineral. Rec.* **22**, 421-425.

EDWARDS, R., GILLARD, R.D., WILLIAMS, P.A. & POLLARD, A.M. (1992): Studies of secondary mineral formation in the PbO–H_2O–HCl system. *Mineral. Mag.* **56**, 53-65.

FLINK, G. (1923): Über die Långbansgruben als Mineralvorkommen. *Z. Kristallogr.* **58**, 356-385.

_____ (1924): Om sarkinit från Långban, ett för fyndorten nytt mineral. *Geol. Fören. Stockholm Förh.* **46**, 661-670.

GREW, E.S., PEACOR, D.R., ROUSE, R.C., YATES, M.G., SU, SHU-CHUN & MARQUEZ, N. (1996): Hyttsjöite, a new complex layered plumbosilicate with unique tetrahedral sheets from Långban, Sweden. *Am. Mineral.* **81**, 743-753.

_____, YATES, M.G., BELAKOVSKIY, D.I., ROUSE, R.C., SU, SHU-CHUN & MARQUEZ, N. (1994): Hyalotekite from reedmergnerite-bearing peralkaline pegmatite, Dara-i-Pioz, Tajikistan and from Mn skarn, Långban, Värmland, Sweden: a new look at an old mineral. *Mineral. Mag.* **58**, 285-297.

HOLTSTAM, D. & MANSFELD, J. (2001): Origin of a carbonate-hosted Fe–Mn–(Ba–As–Pb–Sb–W) deposit of Långban-type in central Sweden. *Mineral. Deposita* **36**, 641-657.

JARL, L.-G. & JOHANSSON, Å. (1988): U–Pb zircon ages of granitoids from the Småland–Värmland granite porphyry belt, southern and central Sweden. *Geol. Fören. Stockholm Förh.* **110**, 21-28.

JAXEL, R. & GELAUDE, P. (1986): New mineral occurrences from the Laurium slags. *Mineral. Rec.* **17**, 183-190.

JONSSON, E. & BOYCE, A.J. (1999): Correlation of mineral parageneses with S and O isotopic variation in Pb–Mn–As–Sb-bearing veins at Långban, Sweden. *In* Mineral Deposits: Processes to Processing (C. J. Stanley *et al.*, eds). Balkema, Rotterdam, The Netherlands (951-954).

KETEFO, E. (1989): Compositional variations and stability conditions of natural and synthetic Mn-bearing micas and olivines of Långban-type. *Medd. Stockholms Univ., Geol. Inst*. **276**.

LUNDSTRÖM, I. (1995): Beskrivning till berggrundskartan Filipstad SO och NO. *Sver. Geol. Unders. ser. Af* **177/185**.

_____ (1999): General geology of the Bergslagen ore region. *In* Långban: the Mines, their Minerals, Geology and Explorers (D. Holtstam & J. Langhof, eds.). Raster Förlag, Stockholm, Sweden (19-27).

MAGNUSSON, N.H. (1924): Långbansmineralen från en geologisk synpunkt. *Geol. Fören. Stockholm Förh.* **46**, 284-300.

_____ (1930): Långbans malmtrakt. *Sver. Geol. Unders. ser. Ca* **23**.

MOORE, P.B. (1970): Mineralogy and chemistry of Långban-type deposits in Bergslagen, Sweden. *Mineral. Rec.* **1**, 154-172.

NYSTEN, P., HOLTSTAM, D. & JONSSON, E. (1999): The Långban minerals. *In* Långban: the Mines, their Minerals, Geology and Explorers (D. Holtstam & J. Langhof, eds.). Raster Förlag, Stockholm, Sweden (89-183).

OAKES, C.S., BODNAR, R.J. & SIMONSON, J.M. (1990): The system NaCl–$CaCl_2$–H_2O. I. The ice liquidus at 1 atm total pressure. *Geochim. Cosmochim. Acta* **54**, 603-610.

OEN, I.S. & WIKLANDER, U. (1982): Isotopic age determinations in Bergslagen, Sweden. III. The Hyttsjö suite of gabbro-diorites and tonalites-granites, Filipstad area. *Geol. Mijnb.* **61**, 309-312.

PAGE, L.M., STEPHENS, M.B. & WAHLGREN, C.-H. (1996): $^{40}Ar/^{39}Ar$ geochronological constraints on the tectonothermal evolution of the Eastern Segment of the Sveconorwegian Orogen, south-central Sweden. *In* Precambrian Crustal Evolution in the North Atlantic Region (T.S. Brewer, ed.). *Geol. Soc., Spec. Publ.* **112**, 315-330.

POTY, B., LEROY, J. & JACHIMOVISZ, L. (1976): Un nouvel appareil pour la mesure de températures sous le microscope: l'installation de microthermométrie Chaixmeca. *Bull. Soc. Fr. Minéral. Cristallogr.* **99**, 182-186.

REED, M.H. & SPYCHER, N.F. (1985): Boiling, cooling and oxidation in epithermal systems: a numerical modeling approach. *In* Geology and Geochemistry of Epithermal Systems (B.R. Berger & P.M. Bethke, eds.). *Rev. Econ. Geol.* **2**, 249-272.

RIMSTIDT, J.D. (1997): Gangue mineral transport and deposition. *In* Geochemistry of Hydrothermal Ore Deposits (H.L. Barnes, ed., 3rd edition). John Wiley & Sons, New York, N.Y. (487-515).

ROEDDER, E. (1984): Fluid inclusions. *Rev. Mineral.* **12**.

SAMSON, I.M. & WALKER, R.T. (2000): Cryogenic Raman spectroscopic studies in the system NaCl–$CaCl_2$–H_2O and implications for low-temperature phase behavior in aqueous fluid inclusions. *Can. Mineral.* **38**, 35-43.

SCHNORRER-KÖHLER, G. (1980): Mendipit $Pb_3Cl_2O_2$ – Neufund für Laurion, Griechenland. *Aufschl.* **31**, 153-155.

SCOTT, A.-M. & WATANABE, Y. (1998): "Extreme boiling" model for variable salinity of the Hokko low-sulfidation epithermal Au prospect, southwestern Hokkaido, Japan. *Mineral. Deposita* **33**, 568-578.

SCOTT, K.M. (1994): Lead oxychlorides at Elura, western NSW, Australia. *Mineral. Mag.* **58**, 336-338.

SEWARD, T.M. (1984): The formation of lead(II) chloride complexes to 300°C: a spectrophotometric study. *Geochim. Cosmochim. Acta* **48**, 121-134.

_____ & BARNES, H.L. (1997): Metal transport by hydrothermal ore fluids. *In* Geochemistry of Hydrothermal Ore Deposits (H.L. Barnes, ed.; 3rd edition). John Wiley & Sons, New York, N.Y. (435-486).

SHEPHERD, T.J., RANKIN, A.H. & ALDERTON, D.H.M. (1985): *A Practical Guide to Fluid Inclusion Studies.* Blackie, Glasgow, U.K.

SJÖGREN, A. (1886): Mineralogiska notiser XII. Fynd af Allaktit i Långbans grufvor. *Geol. Fören. Stockholm Förh.* **8**, 473-474.

_____ (1887): Allaktit från Långbans grufvor. *Öfvers. Kongl. Vetenskaps-Akad. Förh.* 1887, **3**, 107-113.

SJÖGREN, H. (1905): Om kristalliserad pyrochroit från Långbans grufvor. *Geol. Fören. Stockholm Förh.* **27**, 37-41.

_____ (1910): The Långban mines. *Geol. Fören. Stockholm Förh.* **32**, 1295-1325.

SKINNER, B.J. & LUCE, F.D. 1971: Stabilities and compositions of α-domeykite and algodonite. *Econ. Geol.* **66**, 133-139.

SUNDIUS, N. (1963): Rhodochrosite from Långban. *Ark. Mineral. Geol.* **3**, 293-295.

TIBERG, H.V. (1905): Långväga jordskalf eller hvad? *Geol. Fören. Stockholm Förh.* **21**, 94-107.

_____ (1910): Från Geologkongressens malmfältsexkursion. *Värml. Bergsmannaför. Annaler* **1910**, 157-188.

WAHLGREN, C.-H., CRUDEN, A.R. & STEPHENS, M.B. (1994): Kinematics of a major fan-like structure in the eastern part of the Sveconorwegian orogen, Baltic Shield, south-central Sweden. *Precamb. Res.* **70**, 67-91.

WALKER, R.T. & SAMSON, I.M. (1998): Cryogenic Raman spectroscopic investigations of fluid inclusions in the NaCl–$CaCl_2$–H_2O system. *Int. Mineral. Assoc., 17th General Meet.* (*Toronto*), *Abstr. Vol.*, A33.

WEBSTER, J.G. (1990): The solubility of As_2S_3 and speciation of As in dilute and sulphide-bearing fluids at 25 and 90°C. *Geochim. Cosmochim. Acta* **54**, 1009-1017.

Received April 10, 2001, revised manusript accepted December 4, 2001.